Ligand-Induced Polymerization†

Lawrence W. Nichol* and Donald J. Winzor

ABSTRACT: Three models of ligand-induced polymerization are considered, encompassing dimerization of acceptor–ligand complex and cross-linking of monomer units via a ligand bridge to form either dimer or linear chains. For each model a binding equation is developed and examined in terms of limits, form, and intersection within a family of curves, each member constructed with fixed but different total acceptor concentration. The characteristics of the binding curves that emerge are correlated with those found by examining the dependence on ligand concentration of either the weight-average molecular weight of the acceptor constituent or a function of it. In the latter plots, a maximum exists for the cross-linking models at the same ligand concentration that the corresponding binding curves intersect: the existence of the maximum implies that at saturating concentrations of ligand only monomeric acceptor constituent remains. The practical implication of these findings is discussed in terms of experimental systems reported previously in the literature. In addition, particular comment is made on the forms of binding curves for the three models, which assume shapes generally associated with positive and negative cooperativity. Finally, comparison is made with those systems in which a shift toward polymeric constituent is effected by ligand perturbation of a preexisting association equilibrium.

There are several protein (acceptor) systems for which the addition of a specific ligand increases the apparent weight-average molecular weight of the acceptor constituent. The phenomenon is well understood for those systems in which the protein exists as a mixture of polymeric forms in the absence of ligand, the addition of which imposes a constraint on this equilibrium (Nichol et al., 1967; Nichol and Winzor, 1972; Baghurst and Nichol, 1975), but the possibility also exists that the ligand induces polymerization, which does not occur in its absence. Despite the current usage of the term ligand-induced polymerization (Levitski and Koshland, 1972) the latter systems have been relatively unexplored in mathematical terms. In particular, little is understood of the forms of binding curves and their dependence on acceptor concentration, or on the functional relationship between the weight-average molecular weight of acceptor and ligand concentration. It is the purpose of this work to explore these aspects with systems in which ligand-induced polymerization occurs by an indefinite or discrete set of cross-linking reactions.

Theory

Dimerization of an Acceptor–Ligand Complex. Consider first a system in which an acceptor A and a ligand E interact in solution to form an AE complex that dimerizes.

$$A + E \rightleftharpoons AE;\ K_1 = [AE]/[A][E] \qquad (1a)$$

$$2AE \rightleftharpoons A_2E_2;\ K_2 = [A_2E_2]/[AE]^2 \qquad (1b)$$

Equilibrium constants are expressed on a molar scale. It follows that the total concentrations of ligand and acceptor may be expressed as

$$[\bar{E}] = [E] + K_1[A][E] + 2K_1^2K_2[A]^2[E]^2 \qquad (2a)$$

$$[\bar{A}] = [A] + K_1[A][E] + 2K_1^2K_2[A]^2[E]^2 \qquad (2b)$$

The experimentally determinable binding function r, expressed as moles of ligand bound per base-mole of acceptor, then becomes

$$r = K_1[E](1 + 2K_1K_2[A][E])/\{1 + K_1[E] + 2K_1^2K_2[A][E]^2\} \qquad (3)$$

where [A] may be expressed as an explicit function of K_1, [$\bar{A}$], and [E] by solving the quadratic eq 2b. Figure 1 was constructed on the basis of eq 3 using three different values of the dimensionless parameter $K_2[\bar{A}]$. Deviations from linearity in this family of curves show that the corresponding plots of r vs. [E], the limit of r as [E] $\rightarrow \infty$ being 1, are not rectangular hyperbolae, and indeed the appearance of a maximum for the systems with higher $K_2[\bar{A}]$ values is associated with pronounced sigmoidality of the binding curves. Moreover, the curves do not intersect and acceptor-concentration dependence is apparent, characteristics which may be shown from eq 3 to apply generally. The latter characteristics are not unique to the model specified in eq 1, since they also apply to particular cases of the system discussed by Nichol et al. (1967), where the acceptor dimerizes ($2A \rightleftharpoons C$) in the absence of E, which on its addition binds to p and q sites on A and C, respectively, with intrinsic binding constants K_A and K_C. Thus, it may be shown from eq 7 of Nichol et al. (1967) that the point of intersection of binding curves obtained with different [$\bar{A}$] values is given by

$$[E] = (2pK_A - qK_C)/K_AK_C(q - 2p) \qquad (4a)$$

$$r = (2pK_A - qK_C)/2(K_A - K_C) \qquad (4b)$$

For the case $q = 2p$, for example, it is clear that no such point of intersection can exist: moreover, numerical examples with $p = 1, q = 2, K_C > K_A$ have shown that the family of binding curves resembles in form those shown in Figure 1, but with that referring to the smallest [$\bar{A}$] the most sigmoidal.

For both types of system discussed above, the apparent weight-average molecular weight of acceptor will increase on the addition of effector. It is, however, possible by studying the acceptor alone to evaluate the equilibrium constant, $X = [C]/[A]^2$, by a method such as sedimentation equilibrium or (at greater dilutions) frontal gel chromatography (Nichol and Winzor, 1972). If $X = 0$ (no dimer present), a ligand-induced

† From the Department of Physical Biochemistry, John Curtin School of Medical Research, Australian National University, Canberra, A.C.T. 2601, Australia (L.W.N.), and the Department of Biochemistry, University of Queensland, St. Lucia, Qld. 4067, Australia (D.J.W.). *Received August 13, 1975.* This investigation was supported in part by the Australian Research Grants Committee.

[1] Abbreviations used are: EDTA, (ethylenedinitrilo)tetraacetic acid; ATP, adenosine 5′-triphosphate; UTP, uridine triphosphate.

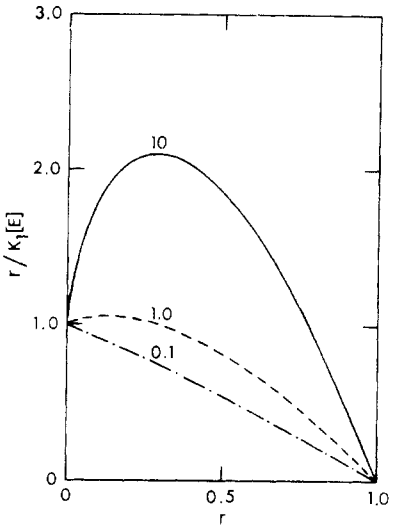

FIGURE 1: Simulated Scatchard plots for a system in which an acceptor A and ligand E interact to form an AE complex that dimerizes (eq 1). The number adjacent to each curve denotes the value of $K_2[\bar{A}]$ used in the computation of data from eq 3.

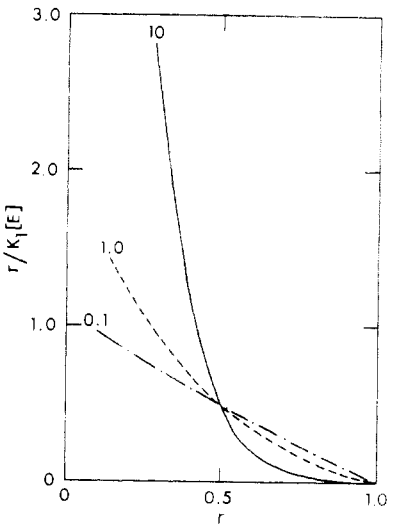

FIGURE 2: Simulated Scatchard plots for a system in which ligand E forms a bridge between two acceptor molecules to form the complex AEA (eq 8). The number adjacent to each curve denotes the value of $K_2[\bar{A}]$ used in the computation of data from eq 9.

polymerization must operate, eq 1 providing one example of this. If $X \neq 0$, then acceptor–ligand mixtures comprise thermodynamically distinct systems, since the additional species (unbound dimer) is now present at equilibrium. In the latter case, even if a cyclic array of equilibria operate including the reactions specified in eq 1, three equilibrium constants suffice to describe the system (provided binding sites on monomer and separately on dimer are equivalent and independent): we choose the experimentally accessible constants X, K_A, and K_C. The redundancy of additional equilibrium constants pertaining to the cyclic array merely stresses that the formation of particular acceptor–ligand complexes may proceed by alternate pathways that cannot be distinguished by equilibrium binding or molecular weight studies. In these terms the ligand-induced and preexisting acceptor equilibrium cases may be distinguished and specified by $X = 0$ and $X \neq 0$, respectively: it remains to discuss evaluation of the respective constants K_1, K_2 ($X = 0$), and K_A, K_C ($X \neq 0$).

First estimates may be obtained by determining the apparent weight-average molecular weight of the acceptor constituent, $\bar{M}_P$, with fixed $[\bar{A}]$ and varying $[\bar{E}]$ (Nichol et al., 1972; Baghurst and Nichol, 1975) as a function of $[E]$, available from prior equilibrium dialysis. Values of $\bar{M}_P$ together with the molecular weight of A, M_A, may be used to formulate the function

$$X^* = M_A(\bar{M}_P - M_A)/\{2[\bar{A}](2M_A - \bar{M}_P)^2\} \quad (5)$$

It may readily be shown by defining $\bar{M}_P$ and $[\bar{A}]$ in terms of the equilibrium concentrations of species present (which differ for the two systems under discussion), and by assuming that $M_E \ll M_A$, that use of eq 5 leads to

$$X^* = \frac{[A_2E_2]}{([A] + [AE])^2} = \frac{K_1^2K_2[E]^2}{(1 + K_1[E])^2} \quad (6a)$$

$$(1/\sqrt{X^*}) = (1/[E]K_1\sqrt{K_2}) + (1/\sqrt{K_2}) \quad (6b)$$

for $X = 0$, the ligand-induced system; and

$$X^* = X(1 + K_C[E])^q/(1 + K_A[E])^{2p} \quad (7a)$$

$$(1/\sqrt{X^*}) = \{(1 + K_A[E])/(1 + K_C[E])\}^p/\sqrt{X};\ q = 2p \quad (7b)$$

for $X \neq 0$, the preexisting equilibrium system. As for the binding curves for the two systems, plots of X^* vs. $[E]$ exhibit similar qualitative features: both monotonically increase with increasing $[E]$ from the appropriate value of X to finite constant limiting values, K_2 (when $X = 0$) and $X(K_C/K_A)^{2p}$ (when $X \neq 0$). The absence of a turning point in each case has been verified by differentiating eq 6a and 7a with respect to $[E]$. However, from plots of $1/\sqrt{X^*}$ vs. $1/[E]$ it is clear from eq 6b and 7b that the systems may be further distinguished, the linear plot for eq 6b ($X = 0$) leading to the direct determination of K_1 and K_2, and the curvilinear plot of eq 7b ($X \neq 0$) providing information additional to binding data from which estimates of p, K_A and K_C may be obtained. It is not claimed, however, that values of X^* or r will be sufficiently precise in an experimental context to permit accurate determination of the relevant equilibrium constants: this could proceed by performing sedimentation equilibrium experiments on acceptor–effector mixtures, whereupon the initial study in conjunction with computer-simulation procedures (Howlett et al., 1970; Howlett and Nichol, 1972; Baghurst and Nichol, 1975), which require a choice of model and first estimates of equilibrium constants, could be used to refine values of the relevant parameters.

Cross-Linking of Acceptor by Bivalent Ligand. The simplest example of this may be represented as

$$A + E \rightleftharpoons AE;\ K_1 = [AE]/[A][E] \quad (8a)$$

$$AE + A \rightleftharpoons AEA;\ K_2 = [AEA]/[AE][A] \quad (8b)$$

for which the binding equation is

$$r = \frac{3K_1[E] - 1 + \{(1 + K_1[E])^2 + 8K_1K_2[\bar{A}][E]\}^{1/2}}{2[K_1[E] + 1 + \{(1 + K_1[E])^2 + 8K_1K_2[\bar{A}][E]\}^{1/2}]} \quad (9)$$

Equation 9 may be used to establish that as $[E] \rightarrow \infty$, $r \rightarrow 1$ and that a family of binding curves constructed with varying $K_2[\bar{A}]$ all intersect at the point ($r = 0.5$, $[E] = 1/K_1$). This behavior is illustrated in Figure 2 which in form (that generally attributed to negative cooperativity) and with the point of intersection exhibits markedly contrasting behavior to that shown in Figure 1. However, ambiguity of interpretation may again arise, since acceptor-concentration dependence and intersec-

tion of binding curves of the same form as those shown in Figure 2 are also predicted for the preexisting polymerization case ($X \neq 0$) when $q < 2p$ and $K_C > 2pK_A/q$, conditions applicable to the binding of organic phosphates to methemoglobin A at pH 5.4 (Baghurst and Nichol, 1975). Indeed, it could be noted that the conditions satisfy eq 4 in defining real and positive coordinates for the point of intersection. In certain respects the behavior of X^* (evaluated from eq 5) vs. [E] curves also parallel each other for the two different systems. For the crosslinking model proposed in eq 8, $X^* = K_1K_2[E]/(1 + K_1[E])^2$, which on differentiation shows that $dX^*/d[E] = 0$ only when $[E]_c = 1/K_1$. This single turning point (a maximum) corresponds to the maximum in a plot of [AEA] vs. [E], the value of [AEA] decreasing to zero as $[E] \rightarrow \infty$. This is consistent with the finding that the limiting value of r is 1, since as $[E] \rightarrow \infty$ all of the acceptor is converted to the AE form. Correspondence between the abscissa value of the maximum ($[E]_c = 1/K_1$) and the position of the point of intersection of the binding curves is also noted. This correspondence also applies to the preexisting polymerization case ($X \neq 0$, $q < 2p$, $K_C > 2pK_A/q$), since Baghurst and Nichol (1975) have shown that a maximum in the X^* vs. $[E]$ plot occurs at the point X_c^* given by their eq 7 and $[E]_c$ given by the same expression as eq 4a. These similarities stress the importance of distinguishing between the quite different systems by prior studies on acceptor alone before attempts are made to obtain first estimates of the appropriate equilibrium constants. If X proves to be equal to zero (the cross-linking model of eq 8), K_1 is directly available as the reciprocal of the value [E] at which binding curves for different [$\bar{A}$] intersect or at which a maximum in X^* is observed: K_2 follows from application of eq 9. If $X \neq 0$, evaluation of the relevant binding parameters could proceed by the method illustrated by Baghurst and Nichol (1975), who also showed how first estimates of constants obtained from (X^*, [E]) data could be improved by relating experimental and computer-simulated sedimentation equilibrium results.

Indefinite Association of Acceptor Induced by Bivalent Ligand. The model in eq 8 is simple in that A was considered to be monofunctional toward E. If A and E are both bifunctional, a series of linear polymers with alternating A and E units may coexist in equilibrium, the situation paralleling that of indefinite association of a single solute (Van Holde and Rossetti, 1967). Provided each successive addition of E or A to the chain is governed by the same standard free energy change, a single equilibrium constant (K_1, on a molar scale) suffices to describe the relevant equilibria. It follows, with suitable factorization, that the total base-molar concentration of acceptor is given by

$$[\bar{A}] = [A](1 + K_1[E] + K_1^2[E]^2) \times (1 + 2K_1^2[A][E] + 3K_1^4[A]^2[E]^2 + \ldots) \quad (10a)$$

$$= [A](1 + K_1[E] + K_1^2[E]^2)/(1 - K_1^2[A][E])^2 \quad (10b)$$

Equation 10b follows from eq 10a by setting the infinite series equal to S, whereupon it may be shown that $S(1 - K_1^2[A][E])$ equals a geometric progression with common ratio $K_1^2[A][E]$ and first-term unity. By entirely analogous reasoning it may be shown that

$$[\bar{E}] = [E](1 + K_1[A] + K_1^2[A]^2)/(1 - K_1^2[A][E])^2 \quad (11)$$

Combination of eq 10b and 11 yields

$$r = \frac{K_1[E]\{1 + 2K_1[E] + K_1[A](1 - K_1^2[E]^2)\}}{1 + K_1[E] + K_1^2[E]^2} \quad (12)$$

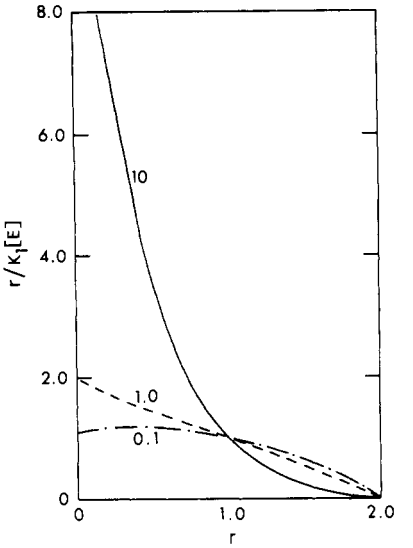

FIGURE 3: Simulated Scatchard plots for a system in which indefinite association of acceptor is induced by ligand cross-links between acceptor units. The number adjacent to each curve denotes the value of $K_1[\bar{A}]$ used in the computation of data from eq 12.

where [A] may be expressed as an explicit function of K_1, [$\bar{A}$], and [E] by solving the quadratic eq 10b. Figure 3 presents binding curves calculated from eq 12 for three values of $K_1[\bar{A}]$. Three points merit comment. First, the limiting value of r is 2, which shows that AE_2 is the sole acceptor species present as $[E] \rightarrow \infty$. Second, all of the binding curves intersect at the point ($r = 1$, $[E] = 1/K_1$): this may be shown generally by substituting $[E] = 1/K_1$ into eq 12. Third, the change in form of the binding curves with $K_1[\bar{A}]$ is quite dramatic: with the largest $K_1[\bar{A}]$ the shape parallels that shown in Figure 2 for the simple cross-linking system; with the smallest $K_1[\bar{A}]$ a maximum is observed in the plot, which like Figure 1 implies sigmoidality of the binding curve; the intermediate behavior observed with the remaining value of $K_1[\bar{A}]$ would be difficult to distinguish experimentally from a rectangular hyperbola in a direct plot of r vs. [E]. Since the switch from apparent negatively cooperative behavior to apparent positive cooperativity may be observed with the same system by suitably varying [$\bar{A}$], an experimenter is in danger of misinterpreting the system from binding results alone, especially if only a single binding curve (at a particular [$\bar{A}$]) is used as the basis of interpretation.

The formulation of X^* from $\bar{M}_P$ data is inappropriate in this case, which would be indicated from binding results in that the limiting value of r is 2, in contrast to the value of unity found with the dimerizing systems (eq 1 and 8). It is possible, however, to write an expression for $\bar{M}_P$ in terms of K_1, [A], and [E], assuming $M_E \ll M_A$, which becomes on cancellation of the common factor

$$\bar{M}_P = \frac{1 + 4K_1^2[A][E] + 9K_1^4[A]^2[E]^2 + 16K_1^6[A]^3[E]^3 + \ldots}{1 + 2K_1^2[A][E] + 3K_1^4[A]^2[E]^2 + 4K_1^6[A]^3[E]^3 + \ldots} \quad (13a)$$

$$= M_A(1 + K_1^2[A][E])/(1 - K_1^2[A][E]) \quad (13b)$$

The closed solution in eq 13b, obtained by summing the infinite converging series in eq 13a, is useful since it may be used with eq 10b to show that a maximum occurs in the plot of $\bar{M}_P$ vs. [E] at $[E] = 1/K_1$, and to construct the plots shown in Figure

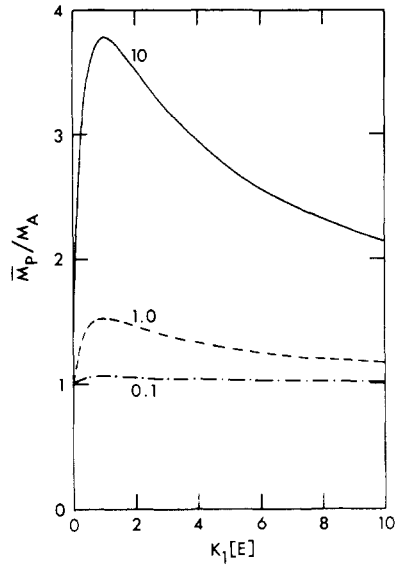

FIGURE 4: Simulated plot of the dependence of the weight-average molecular weight of acceptor constituent for a system undergoing ligand-induced indefinite association. The number adjacent to each curve denotes the value of $K_1[\bar{A}]$ used in the computation of data from eq 13b.

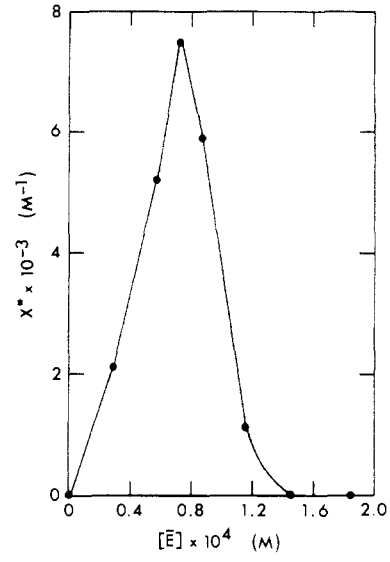

FIGURE 5: Dependence of X^* on total ligand concentration for mixtures of human mercaptalbumin (A) and mercuric chloride (E) in acetate buffer, pH 4.25, I 0.05. The curve, which has no theoretical significance, has been drawn to emphasize the trend of the data, calculated from Figure 6 of Edelhoch et al. (1953) by means of eq 5.

4, which have their binding counterparts in Figure 3. Evidently a first estimate of K_1 could be determined from either the point of intersection of the binding curves (Figure 3) or the maximum position in Figure 4. The importance of conducting a series of experiments at fixed (but different) $[\bar{A}]$ values is also apparent from both Figures, since binding results at a particular $[\bar{A}]$ considered alone are likely to be misinterpreted, as noted earlier.

Discussion

It is timely to consider the behavior of certain experimental systems in relation to the above theory. The interaction of mercaptalbumin with mercuric chloride forms a convenient first example, since it is well-established that mercaptalbumin does not exist as a rapidly equilibrating monomer–dimer system in the absence of ligand (Edelhoch et al., 1953). Moreover, the existence of a single sulfhydryl group per mole of monomer and the bifunctional nature of mercuric chloride almost certainly ensure that the observed ligand-induced dimerization conforms basically to eq. 8. Figure 5 presents a plot of X^* vs. $[\bar{E}]$ for this system, the ordinate values being calculated from eq 5 and the light scattering data from Figure 6 of Edelhoch et al. (1953). The predicted maximum is observed, occurring at an X^* value ($K_2/4$) which indicates that $K_2 = 3.0 \times 10^4$ M^{-1}, in agreement with the value calculated by Edelhoch et al. (1953) on the assumption that $[E] = 0$. The present interpretation does not involve this assumption and, moreover, may be used to test its validity. Thus, for the values of $[\bar{A}]$ and $[\bar{E}]$ appropriate to the maximum the free concentration [E], although not known explicitly, equals $1/K_1$. Accordingly this information may be used to solve the simultaneous equations for $[\bar{A}]$ and $[\bar{E}]$, the result being a value less than 10^{-8} M for [E], which substantiates the previous assumption. It also shows that binding curves cannot be obtained for this system. Finally, we note that equilibrium considerations alone suffice to explain the progressive decrease in concentration of dimeric complex with [E] or $[\bar{E}]$ at high $[\bar{E}]$, but recognize that the detailed mechanism indicated from kinetic studies may well be more complicated (Edelhoch et al., 1953).

A similar ligand-induced dimerization has been proposed for the interaction of Zn^{2+} with α-amylase monomer to form dimer via a Zn^{2+} cross-link (Stein and Fischer, 1960). However, the proportion of dimer, as judged by sedimentation velocity analysis, progressively increases as $[\bar{E}]$ increases (Isemura and Kakiuchi, 1962), and indicates a limiting value of ∞ for X^*: such behavior is at variance with that of discrete or indefinite cross-linking mechanisms. Possible alternative models must be examined in this light and in accord with the finding that whereas monomeric α-amylase contains no zinc, the dimeric species contains 0.5 mol of Zn/base-mole (Stein and Fischer, 1960). The latter observation excludes the model specified in eq 1, which would require a 1:1 stoichiometry. A simple explanation that seems to account for all findings is that α-amylase exists as a mixture of monomeric and dimeric species in the absence of Zn^{2+} and that on addition of Zn^{2+} $p = 0, q = 1$. In this connection it is of interest that α-amylase in the presence of 0.01 M calcium-EDTA dimerizes with an equilibrium constant of 2.4×10^3 M^{-1}, a value deduced from the light-scattering data of Kakiuchi et al. (1965). It is now possible to employ their light-scattering data obtained in the presence of Zn^{2+} (curve V in Figure 4 of Kakiuchi *et al.*, 1965) to obtain X^* (eq 5) and hence K_C from eq 7a: [E] was obtained from $[\bar{E}]$ by similar means to that adopted with the mercaptalbumin system. From five determinations of $\bar{M}_P$, K_C was estimated to be $7.0 \pm 1.0 \times 10^5$ M^{-1}.

The above examples suffice to illustrate a system where ligand in a rigorous sense has induced dimerization and one in which it has merely perturbed a preexisting dimerization. At first sight it might appear that the detection of a ligand-induced polymerization would be facilitated by examining the acceptor in the presence of saturating concentrations of ligand. The findings in this work show that this approach is entirely inappropriate to the study of cross-linking reactions (discrete or indefinite); for with these systems the acceptor would have reverted to monomeric constituent. The approach is valid for the detection of ligand-induced dimerizations represented by eq 1 or in general to systems where ligand perturbs a preexisting monomer–polymer equilibrium (except for the special case $q < 2p$, $K_C > 2pK_A/q$). The fact that some systems examined in the context of ligand-induced polymerization do

exhibit sigmoidal binding curves and are characterized by an infinite value of X^* (or its equivalent) at saturating ligand concentrations strongly suggests that these too may belong to the preexisting equilibrium category. Examples include the binding of threonine to the aspartokinase-homoserine dehydrogenase system (Janin and Cohen, 1969; Wampler et al., 1970) and of ATP or UTP to cytosine triphosphate synthetase (Levitzki and Koshland, 1972). Two final points may be made. First, despite the apparent similarity in experimental behavior of alternative models, mathematical expressions are now available which permit computer-simulation of, for example, binding curves and hence distinction in quantitative terms between possible alternatives. The second and related point is that it is hazardous to ascribe mechanistic significance to the form of a binding curve merely on the grounds that it exhibits apparent positive or negative cooperativity.

References

Baghurst, P. A., and Nichol, L. W. (1975), *Biochim. Biophys. Acta 412,* 168.

Edelhoch, H., Katchalski, E., Maybury, R. H., Hughes, W. L., Jr., and Edsall, J. T. (1953), *J. Am. Chem. Soc. 75,* 5058.

Howlett, G. J., and Nichol, L. W. (1972), *J. Biol. Chem. 247,* 5681.

Howlett, G. J., Jeffrey, P. D., and Nichol, L. W. (1970), *J. Phys. Chem. 74,* 3607.

Isemura, T., and Kakiuchi, K. (1962), *J. Biochem. (Tokyo) 51,* 385.

Janin, J., and Cohen, G. N. (1969), *Eur. J. Biochem. 11,* 520.

Kakiuchi, K., Hamaguchi, K., and Isemura, T. (1965), *J. Biochem. (Tokyo) 57,* 167.

Levitzki, A., and Koshland, D. E., Jr. (1972), *Biochemistry 11,* 247.

Nichol, L. W., Jackson, W. J. H., and Winzor, D. J. (1967), *Biochemistry 6,* 2449.

Nichol, L. W., Jackson, W. J. H., and Winzor, D. J. (1972), *Biochemistry 11,* 585.

Nichol, L. W., and Winzor, D. J. (1972), Migration of Interacting Systems, Oxford, Clarendon Press.

Stein, E. A., and Fischer, E. H. (1960), *Biochim. Biophys. Acta 39,* 287.

Van Holde, K. E., and Rossetti, G. P. (1967), *Biochemistry 6,* 2189.

Wampler, D. E., Takahashi, M., and Westhead, E. W. (1970), *Biochemistry 9,* 4210.

Histone Interactions in Solution and Susceptibility to Denaturation†

Dennis E. Roark,* Thomas E. Geoghegan,‡ George H. Keller, Karl V. Matter, and Richard L. Engle

ABSTRACT: Histone interactions in solution may depend upon treatments used for purification. Optical rotatory dispersion and sedimentation-velocity measurements have been made in a reference solvent, before and after exposure to various treatments, to investigate histone susceptibility to irreversible denaturation. Some acid conditions and urea and guanidine solutions may denature. Interaction studies performed on nondenatured histones indicate that the dimer, (H4)(H3), and tetramer, $(H4)_2(H3)_2$, dissociate to monomers at low ionic strength. Sedimentation-velocity experiments suggest a model for the $(H4)_2(H3)_2$ tetramer, with a compact semispherical center and four protruding amino-terminal regions. Fractions H2a and H2b interact to form the mixed dimer in equilibrium with monomers. Fraction H2a self-associates readily to dimers, tetramers, and octamers, while fraction H1 associates only weakly to form dimers.

Histone interactions play an essential role in the maintenance of chromatin structure. The role may be that of packaging the DNA and/or nonspecific mediation of the regulation of transcription or replication. Recent studies have begun to describe the structural features of nucleoprotein. Chromatin subfragments have been visualized by electron microscopy of cross-linked chromatin (Olins and Olins, 1974), and isolated following nuclease digestion (Hewish and Burgoyne, 1973; Sahasrabuddhe and van Holde, 1974; Noll, 1974; and Oosterhof et al., 1975). Kornberg (1974) has suggested that these subfragments are the primary structural unit of chromatin and contain two each of histones H4, H3, H2a, and H2b. Partial cross-linking of histones bound to DNA has indicated the proximity of histones H4, H3, H2a, and H2b (Martinson and McCarthy, 1975; Hyde and Walker, 1975; and van Lente et al., 1975); indeed, Thomas and Kornberg (1975) have identified the octamer containing two each of these four histones. These proximal histones interact both with DNA and with each other. Studies of isolated histones in solution may be used to investigate histone-histone interactions. The cross-linking of DNA-bound histones and the solution studies complement each other in that the former elucidates the chromatin structure, while the latter identifies specific histone interactions contributing to that structure.

Solution studies have demonstrated several pairs of histone interactions. We have previously reported the existence of an H4–H3 complex which reversibly self-associates to form the $(H4)_2(H3)_2$ tetramer (Geoghegan et al., 1974; Roark et al., 1974; Roark, 1976). The tetramer has been observed in the similar solution studies of Kornberg and Thomas (1974) and

† From the Department of Biological Chemistry, The Milton S. Hershey Medical Center, The Pennsylvania State University, Hershey, Pennsylvania 17033. *Received September 30, 1975.* Supported by the United States Public Health Service Grant GM18456.

* Present address: Departments of Physics and Biology, Maharishi International University, Fairfield, Iowa 52556.

‡ Present address: Department of Biochemistry and Pharmacology, Tufts University School of Medicine, Boston, Mass. 02111.